

Review of Microscopy

Topic 1. We used geometrical (ray) optics to understand how a converging lens forms an image and how two converging lenses generate magnification in a rudimentary compound microscope. A converging lens creates two kinds of images – real and virtual. Real images are generated when the object distance exceeds the focal length, f . In this case, the divergence of the rays does not exceed the lens's ability to convert diverging waves into converging waves, and light is brought to focus in the image plane. Virtual images are generated when the object distance is less than f , and thus the divergence of the rays exceeds the lens's ability to bring the light to focus. Despite this, when viewed by the eye, light appears to arise from a virtual image.

The important image-forming attributes of a converging lens are summarized in the table below:

Object Location	Image Type	Image Location	Image Orientation	Image Size Object Size
$\infty > o > 2f$	Real	$f < i < 2f$	Inverted	< 1 (minified)
$o = 2f$	Real	$2f$	Inverted	$= 1$ (same size)
$2f > o > f$	Real	$2f < i < \infty$	Inverted	> 1 (magnified)
$o = f$		$\pm\infty$		
$o < f$	Virtual	$o < i $	Upright	> 1 (magnified)

The results in the table can be verified using two approaches.

Approach 1: Ray tracing, which is illustrated in Figures 1 and 2:

Ray tracing to generate real images

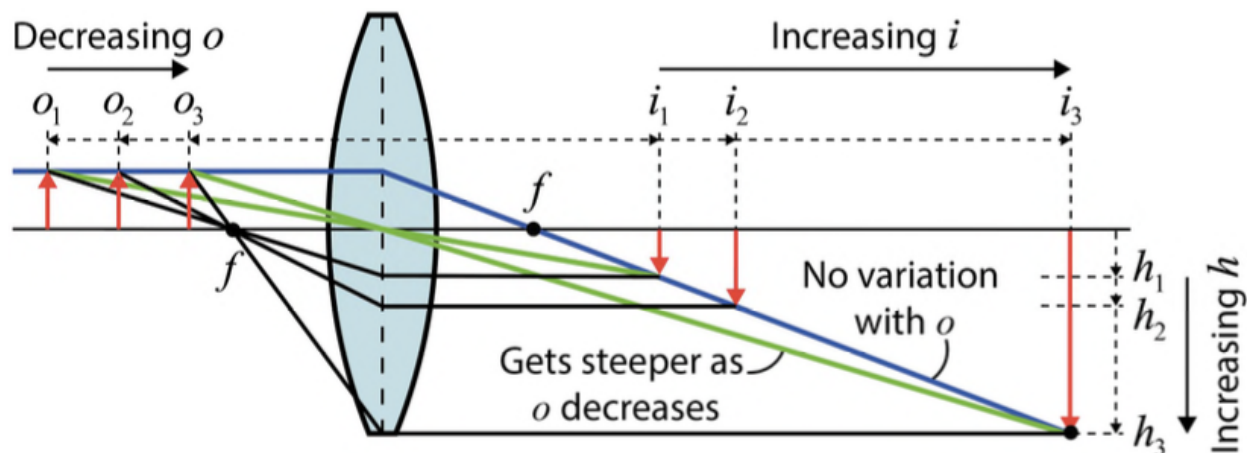


Figure 1

Ray tracing to generate virtual images

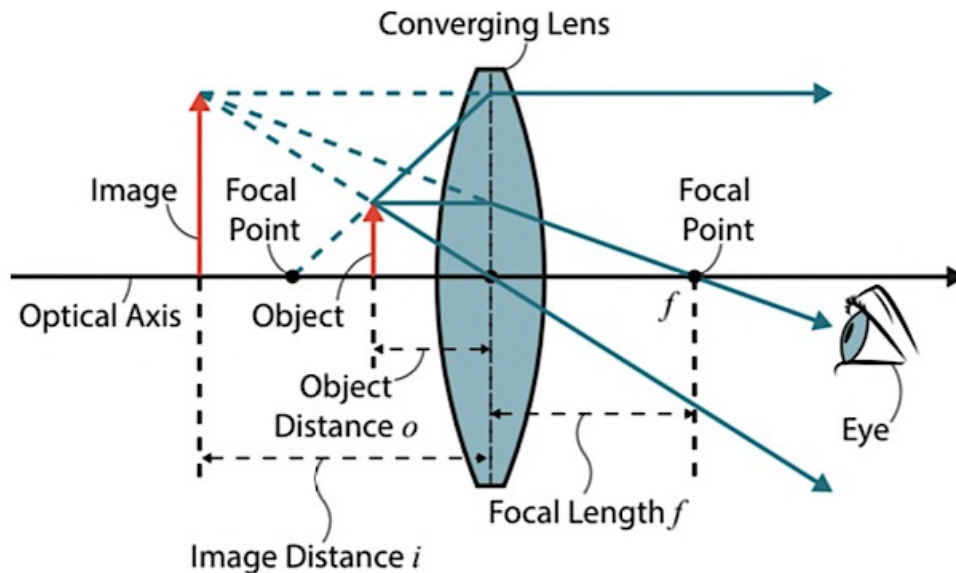


Figure 2

Approach 2: The thin lens equation and the transverse magnification equation, as described below:

Thin Lens: $1/i + 1/o = 1/f$

o = object distance from lens center

i = image distance from lens center

f = focal length

Transverse Magnification: $M_T = -i/o$

When using these equations with a converging lens, the following conventions need to be followed:

f is positive

o is positive (we will ignore virtual objects)

i is positive if the image is real (on the opposite side of the lens from the object and light actually arrives at this location)

i is negative if the image is virtual (on the same side of the lens as the object and light appears to diverge from this location)

M_T is positive if the image is upright and negative if it is inverted

A rudimentary compound microscope is shown in Figure 3. The microscope consists of two lenses. The first lens creates a magnified real inverted image, which becomes the object for the second. The second lens creates a further magnified virtual image, which is viewed by the eye.

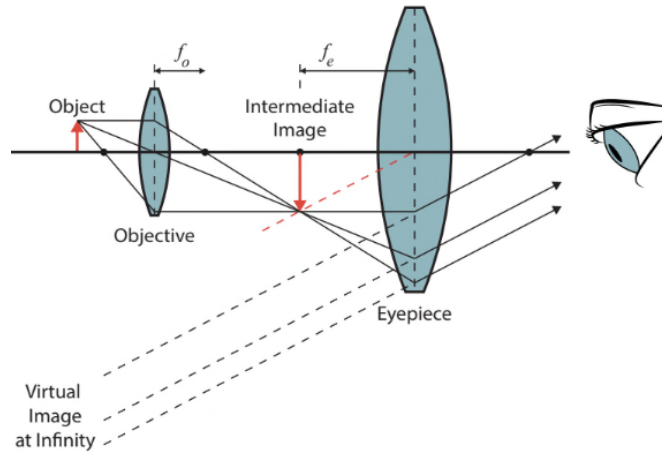


Figure 3

Topic 2. We discussed how to create uniform, partially coherent illumination in the specimen plane. This is accomplished via Köhler's method, which is shown schematically in Figure 4.

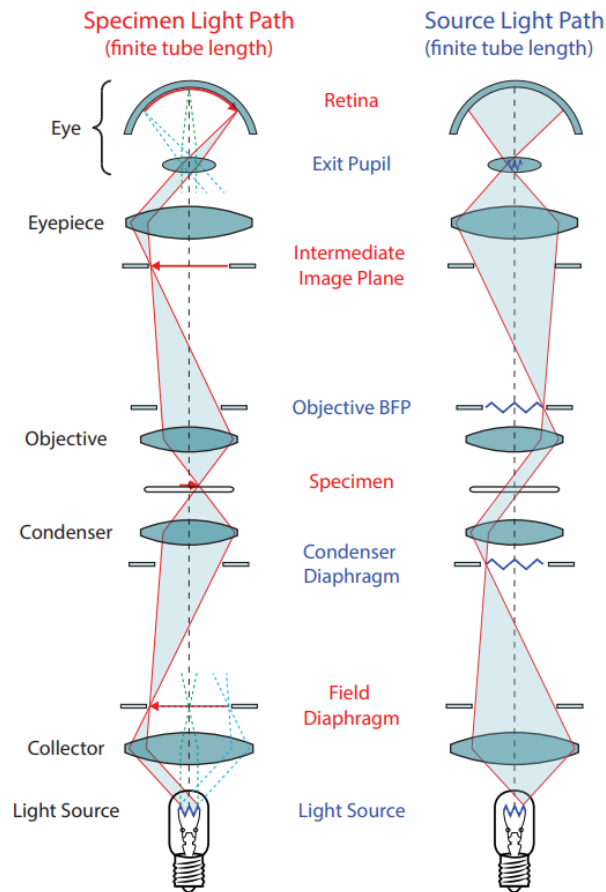


Figure 4

Topic 3. We turned to wave optics to understand how diffraction affects resolution and image formation in optical microscopy.

In geometrical optics, point objects create point images, and light from the object plane is focused on a well-defined image plane. Both of these attributes of image formation are approximate. A more accurate picture is provided by wave optics, which incorporates interference and diffraction into image formation.

One important result from wave optics is that diffraction by apertures causes the image of an incoherent point source to spread over the image plane in the form of an Airy disk. The radius of the Airy disk is given by:

$$r_{\text{Airy}} = 0.61\lambda_0/(NA) \approx \lambda_0/2$$

In this equation, $NA = n \sin \theta$ is the numerical aperture of a lens with a collection half angle of θ , immersed in a medium of refractive index n .

There are two important implications of this equation. The first is that all objects smaller than the Airy disk will appear enlarged, having the size of the Airy disk. The second, which is embodied in the Rayleigh resolution criterion, is that objects that are spaced more closely than $\sim\lambda/2$ will start to merge together and will be difficult to resolve. The resolution limit of optical microscopy thus often is stated to be ~ 200 nm, assuming blue light ($\lambda_0 = 400$ nm).

Another important implication of wave optics was discovered by Ernst Abbe. Abbe studied image formation using diffraction gratings as objects. Under plane perpendicular illumination, a grating with spacing d diffracts light and produces bright spots of constructive interference at angles given by the expression

$$d \sin \theta = m\lambda$$

In this equation, $m = 0, \pm 1, \pm 2, \dots$, where $m = 0$ corresponds to undiffracted light. Abbe studied the diffraction spectra, which are observable in the BFP of the objective, and the grating image in the image plane, and he made a number of key observations and drew a number of important conclusions. These include:

1. If the objective captures only the undiffracted light, the image is unresolved; formation of a resolved image requires capture of at least two spots in the diffraction pattern.
2. Resolution improves with the capture of more diffraction orders.

3. Specimen details with a size on the order of λ diffract light, and interference between this diffracted light and undiffracted light (or two orders of diffracted light) is essential for image formation.
4. The image can be manipulated by spatial filtering, which involves altering the diffraction pattern in the BFP of the objective. For example, when Abbe masked out all spots except $m = 0$ and $m = \pm 2$ from the spectrum of a grating with spacing d , he found that the image was that of a grating of spacing $d/2$.
5. Abbe derived a famous formula for resolution, $\lambda_0/(2NA)$, which is strikingly similar to the Airy/Rayleigh formula.

Topic 4. We discussed the fact that an image needs to possess contrast because the eye detects variations in amplitude (intensity) and color of the electric field. This led naturally into a discussion of six different forms of optical microscopy (Brightfield, Darkfield, Phase Contrast, Polarization, Differential Interference Contrast, and Fluorescence) that rely on different mechanisms to generate contrast. All are reviewed below. It also led to a discussion of spatial filtering, which plays a key role in many contrast enhancement techniques.

Key concepts in spatial filtering are:

1. Undeviated light gives rise to a homogeneous background in the image.
2. Peripheral spots in the diffraction pattern encode fine details/sharp edges in the object, whereas more central spots encode coarser features. Filtering out either peripheral or central spots causes a loss in the image of the features encoded by the filtered spots.

Brightfield

This imaging mode is the most straightforward. The Köhler method is used to illuminate the specimen, which absorbs and diffracts some of the light while passing most undeviated. To generate good contrast using brightfield, the specimen needs to alter the amplitude and/or color of the electric field sufficiently; this is the case with “amplitude” specimens, such as stained cells. The study of stained samples using brightfield imaging is especially important in medical diagnostics, where it is used to identify cancerous cells and bacteria. Unfortunately, clear and colorless specimens, like unstained cells, generate very poor contrast in brightfield and are essentially invisible.

Darkfield

In this imaging mode, specimens become visible in the same way that stars become visible at night – by making the background dark. One way to implement darkfield (shown in Figure 5) is to use a condenser with an NA that exceeds that of the objective and to put a mask in the FFP of the condenser that creates a hollow cone of illumination in the specimen plane. In this case, all of the illuminating rays will miss the objective if there is no specimen, and the field will be dark. In contrast, if a specimen is present, optical discontinuities in the specimen will diffract, refract, and reflect some light into the objective, and a weak signal will be generated that is nevertheless visible because the background is dark. Darkfield works well for thin samples but poorly for thick samples.

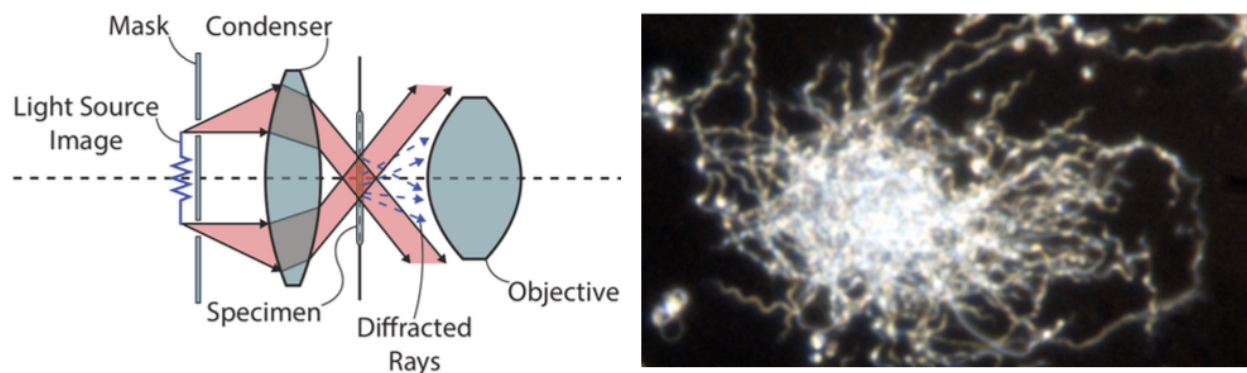


Figure 5

Phase contrast

In this Nobel Prize-winning imaging mode, clear and colorless specimens that alter the phase of the electric field are made visible by converting phase variations, which are not detectable by the eye, into amplitude variations.

The basic idea underlying the technique can be understood by drawing vectors representing the electric fields associated with the undeviated zeroth order (Z) wave, the diffracted (D) wave created by the specimen, and the total specimen (T) wave, which is the sum of Z and D . In the absence of any spatial filtering, the diagram shows that a thin, transparent specimen creates a diffracted wave that is $\sim 90^\circ$ out of phase with the zeroth order wave and of smaller magnitude. D actually lags Z by 90° if the specimen has a higher refractive index than the surroundings because in this case light travels more slowly in the specimen. The key message from the diagram is that the vector representing the T wave has essentially the same length as the vector representing the Z wave. This means that Z and T have the same amplitude and are essentially indistinguishable by the eye, and so a transparent specimen imaged using brightfield is invisible.

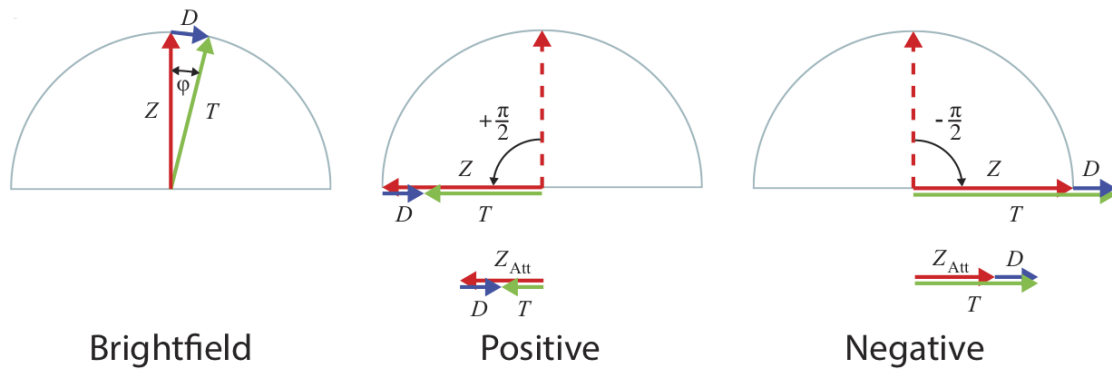


Figure 6

To rectify this problem, Zernike used spatial filtering to advance Z by another 90° .¹ This generates destructive interference between Z and D . The associated vector diagram shows that Z and T now have significantly different lengths and that there thus is amplitude contrast. If the specimen is thin, objects with a refractive index that exceeds that of the surrounding medium appear darker gray against a lighter gray background because T is smaller than Z . Zernike's method is known as positive phase contrast; Z also can be retarded by 90° to generate contrast via constructive interference (negative phase contrast). The ideas underlying phase contrast, its implementation, and its effects on images are illustrated in Figure 7, along with a comparison with brightfield. Also shown is the condenser annulus, which produces annular illumination and which must be aligned with the phase plate.

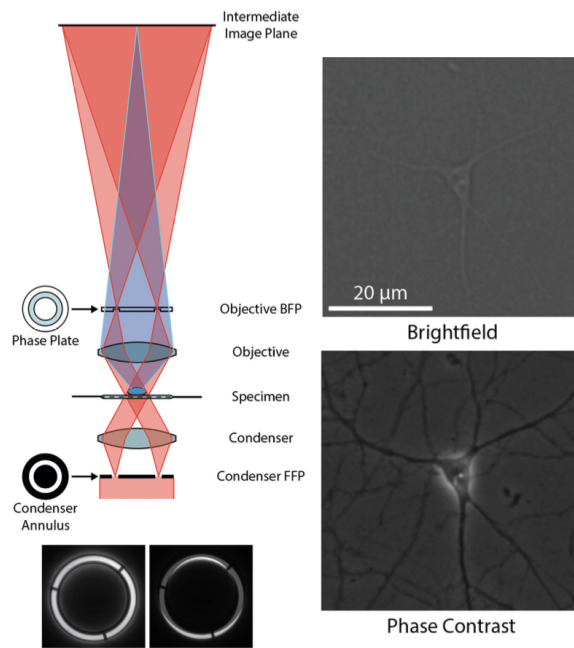


Figure 7

¹ The filter also attenuates the amplitude of Z so it is nearer that of D .

Polarization

In this imaging mode, optical anisotropies in a birefringent specimen are used to create contrast. (A birefringent specimen has refractive indices that depend on direction of ray incidence and light polarization.) Polarization microscopy generates useful images for a restricted, but important, set of biologically relevant structures, such as spindle fibers, red blood cells, and gut granules in *Caenorhabditis elegans*.

In biological polarization microscopy, the birefringent specimen is placed between two polarizers with transmission axes that are orthogonally oriented; these are known as crossed polarizers. The background is dark, but the specimen can generate a signal against the dark background. The effect of the birefringent specimen is analogous to the effect of inserting a third polarizer between crossed polarizers. The intervening polarizer can rotate light polarization and thereby restore signal, as shown in Figure 8.

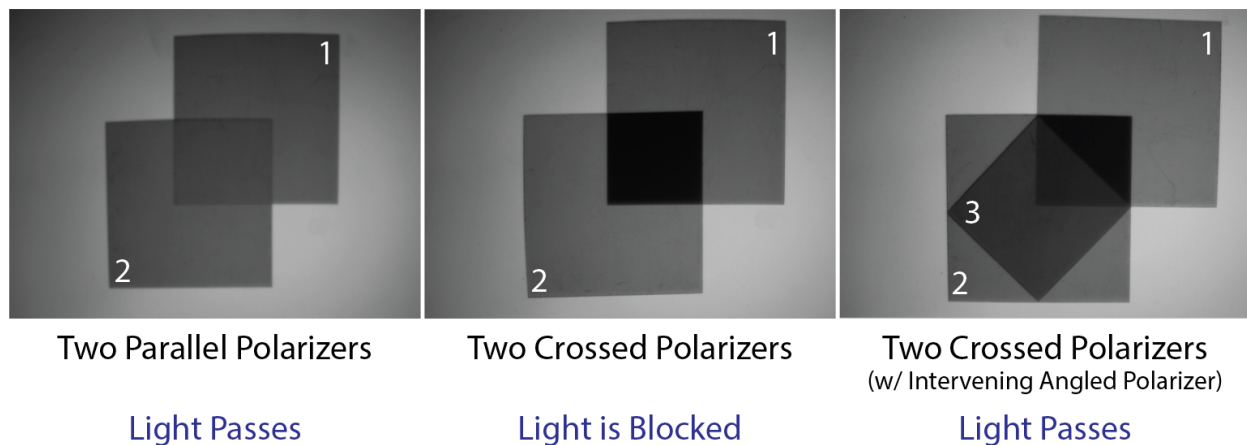


Figure 8

More specifically, contrast generation by the birefringent specimen arises from a specimen-induced change in light polarization.² The specimen typically will produce light with elliptical polarization that will have a component along the transmission axis of the second polarizer, which is known as an analyzer. The transmitted component will generate a specimen-induced signal against the dark background that is a source of contrast. For example, exemplary output polarizations, and the associated amount of light transmitted through the analyzer, are shown for different specimen-induced phase shifts in Figure 9.

² Birefringent specimens can alter light polarization because they split plane polarized light into two linearly polarized, orthogonal, phase-shifted waves that traverse identical regions in the specimen, as shown in Figure 9. The vector sum of these two waves is a new elliptically polarized wave.

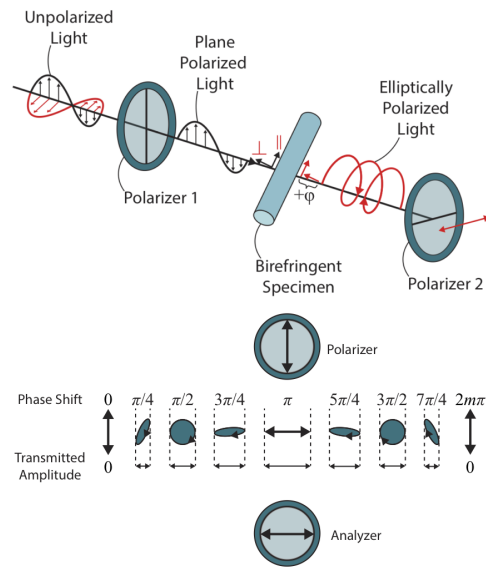


Figure 9

Differential Interference Contrast (DIC)

I skipped DIC this year and will not test on the approach. I have included a brief synopsis for those who are practitioners (or are interested).

In this imaging mode, gradients in the phase lag introduced by the specimen are converted into contrast.

DIC and polarization microscopy are in some respects similar. In both approaches, signal is created when two beams superimpose to generate a beam with a nonzero component along an analyzer. One key difference is that in polarization microscopy the specimen is birefringent and generates the two beams. In DIC, the specimen is not birefringent, and the two beams are generated instead by a birefringent prism.

Another key difference relates to the mechanism of contrast generation. In DIC, a prism generates two independent, slightly laterally shifted ("sheared") waveforms that can be used to create a "double image." Specifically, each waveform traverses the specimen and produces an image, which is an imprint of the phase profile. After traversing the specimen, the two waveforms are reverse laterally shifted ("unsheared"), and thus the two images superimpose slightly out-of-register. The critical consequence of unshearing is that phase differences between the waveforms arise in regions of the specimen containing refractive index gradients, such as edges. Thus, these regions generate elliptical light that can pass the analyzer to create signal, similar to polarization microscopy.

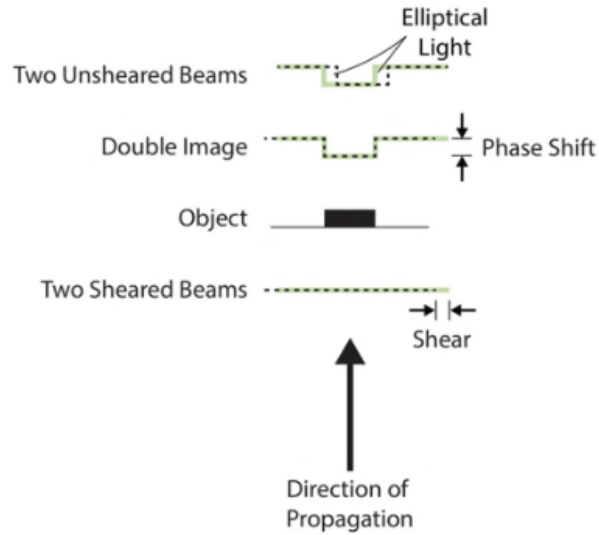


Figure 10

Fluorescence

Fluorescence microscopy has emerged as the dominant form of microscopy in the biological sciences. This is due in large part to the fact that the technique is:

1. Sensitive because $\lambda_{\text{emission}} > \lambda_{\text{excitation}}$, and thus the excitation light can be filtered out and the emission viewed against a dark background.
2. Specific because most molecules do not fluoresce, and thus structures of interest must be specifically tagged with a good fluorophore.
3. Suited to imaging multiple structures within the same specimen using spectrally compatible fluorophores.
4. Compatible with live imaging.

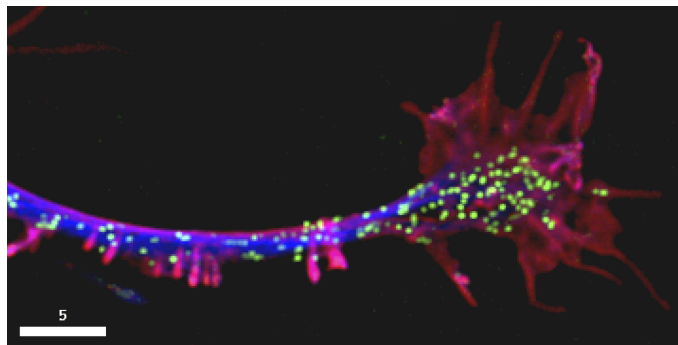


Figure 11

Epifluorescence microscopy is the preferred form of the technique; its attributes are shown in Figure 12. One key component is the dichromatic mirror, which reflects the shorter wavelength excitation light onto the sample and then transmits the longer wavelength emission captured by the objective (which also acts as the condenser) onto the detector.

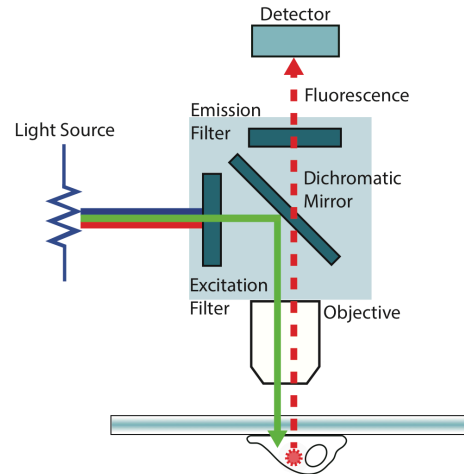


Figure 12

Despite its power, conventional, widefield fluorescence microscopy is plagued by image blur arising from collection of out-of-focus fluorescence.

Topic 5. We ended the section on microscopy with a discussion of a spectrum of approaches to reduce blur and improve resolution in fluorescence images.

Confocal microscopy

(A) *Laser scanning confocal microscopy (LSCM)*. There are two key features of LSCM. The first is illuminating the sample with a focused laser spot. The second is spatial filtering in the intermediate image plane using a pinhole that preferentially passes fluorescence from in-focus parts of the sample. These two features of LSCM markedly reduce blur, which is a major strength of the technique. Weaknesses include slow image acquisition because the beam is scanned across the specimen and reduced signal strength due to the rejection of light.

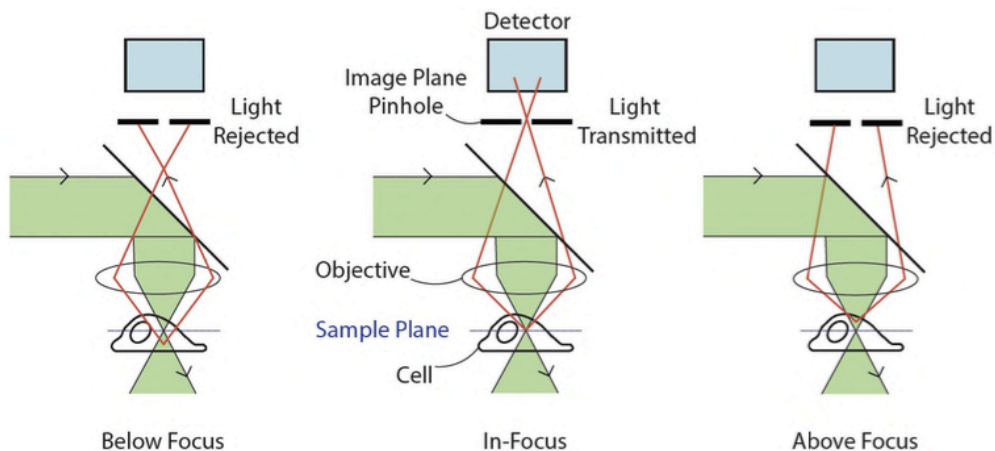


Figure 13

(B) *Spinning disk confocal microscopy (SDCM)*. Much more rapid image acquisition is obtained with SDCM, which is the confocal method of choice for living samples. However, the out-of-focus rejection of spinning disk is somewhat poorer than that of LSCM.

In SDCM systems, the temporal limitations on LSCM are circumvented via multi-beam scanning using a Nipkow disk, which contains tens of thousands of pinholes. Similar to LSCM, the disk and its pinholes are located in a plane conjugate to the sample. A subset of these (~1000) is illuminated, and the objective projects their minified images onto the sample to achieve multi-beam illumination, as shown in Figure 14. The specimen can be scanned in less than a millisecond during a partial rotation of the disk.

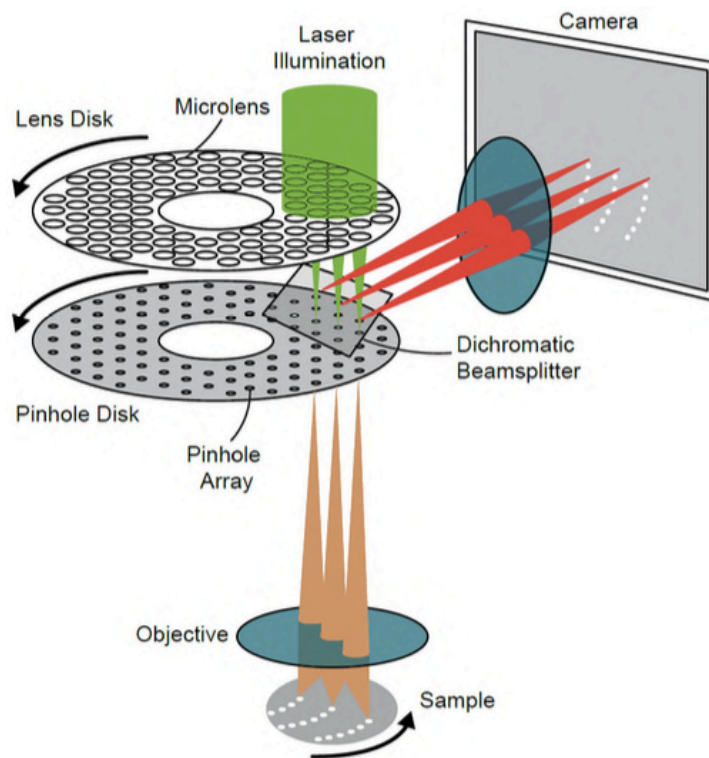


Figure 14

Computational deblurring/deconvolution

This approach achieves results that are very similar to LSCM via a very different methodology. Conventional, blurry widefield fluorescence images are collected, and then the blur is removed computationally based on deconvolution. Deconvolution is founded in the theoretical idea that image blurring can be described by a convolution operation (represented using an \otimes). Stated mathematically, $I = O \otimes PSF$, where I is the blurred image intensity distribution, O

is the object intensity distribution, and the *PSF* is the point spread function (*PSF*) of the microscope.

The goal of computational deblurring is to determine O , and this can be accomplished by determining the *PSF*, which is the image of a point source of light, either theoretically or experimentally. Together with the known image intensity distribution, deconvolution is used to invert the blurring process and reconstruct the object. A theoretical *PSF* and the effect of computational deblurring are shown in Figure 15.

Significant differences between computational deblurring and LSCM are that the former does not require scanning and is not limited to the excitation lines provided by a laser. The computational approach also gives stronger signals from dim specimens because there is no signal rejection. However, the computational approach requires that the *PSF* be accurately determined, usually by experiment, and that a three-dimensional image stack be collected to implement deconvolution correctly. LSCM and computational deblurring can be used together to optimize deblurring.

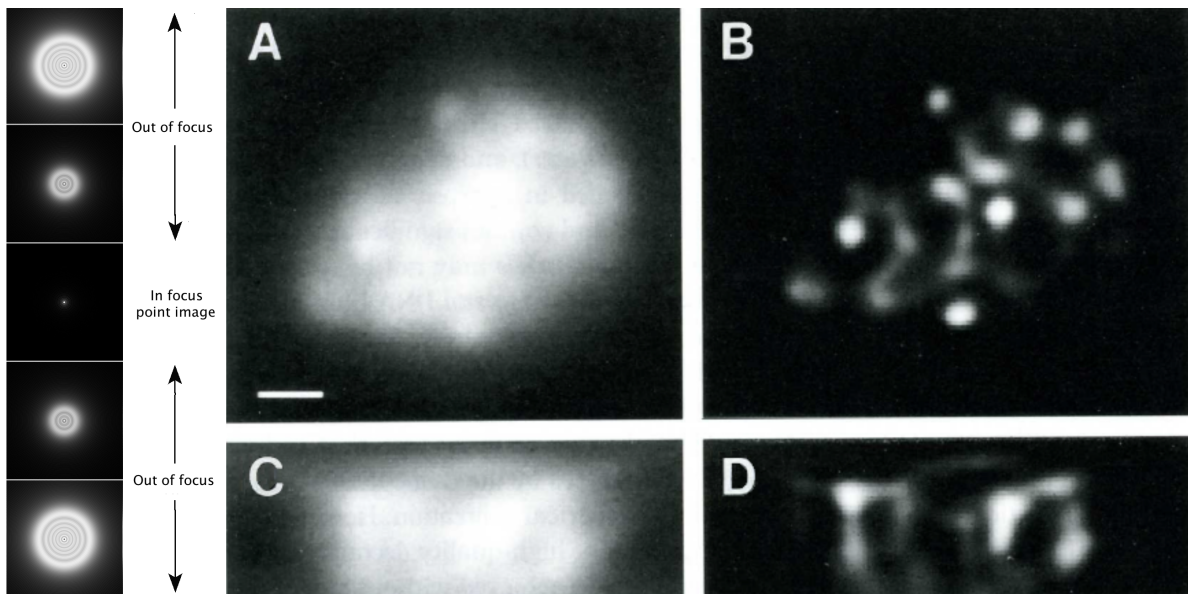


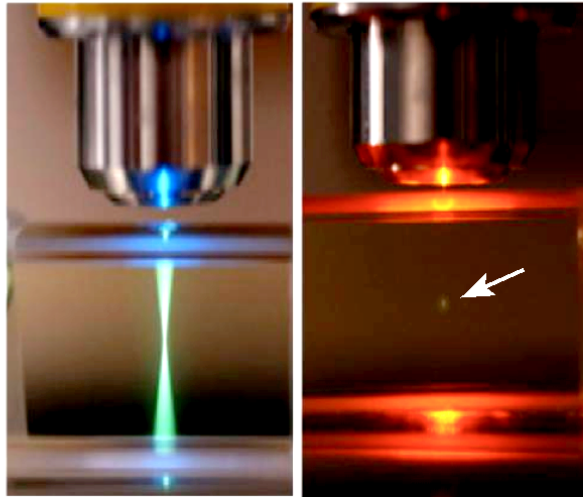
Figure 15

Two photon microscopy

Two-photon microscopy generates exceptionally clear images of objects deep within tissues by confining the region of excitation and emission to a very thin part of the sample, as shown in Figure 16. No pinhole is needed to reject out-of-focus

fluorescence because it is never generated in the first place; there also is minimal bleaching and phototoxicity because excitation is confined to a very thin region.

1-photon vs. 2-photon



Fluorescence from out of focus planes **Fluorescence from focal spot only**

Figure 16

Excitation and emission are severely confined in two-photon imaging because fluorophores are excited via simultaneous absorption of two photons, each having half the energy of a single photon used to induce the transition. For example, in a typical case, a fluorophore that will absorb 600 nm light is instead excited by simultaneous absorption of two 1200 nm (infrared/IR) photons. Two photon absorption is exceedingly unlikely unless the light is very intense because the two photons must both be absorbed within $\sim 10^{-18}$ seconds. The need for high intensity confines excitation and emission to the plane of focus of the laser beam. This, in turn, leads to a marked reduction in negative effects of scattering when imaging deep structures. Two-photon also is the technique of choice for imaging deep structures because IR photons penetrate well.

Total internal reflection fluorescence microscopy (TIRFM)

Unlike two-photon microscopy, which is suited to deep imaging, TIRFM is suited to imaging phenomena near an interface. In biological applications, a glass coverslip and the surface of adherent cells typically create the interface, and TIRFM correspondingly is used to image processes occurring near the cell membrane, such as exocytosis.

TIRFM generates exceptionally clear images of processes near an interface by exploiting unique attributes of the electric field created by TIR. TIR is a process that occurs when light is incident from a region of higher refractive index at sufficiently high angle and reflects off a region of lower refractive index. Geometrical optics predicts “total reflection” under these conditions, and thus no electric field in the lower index medium (e.g., the cell interior). In contrast, wave optics reveals instead that a non-propagating “evanescent” electric field penetrates into the lower index medium, as shown in Figure 17.

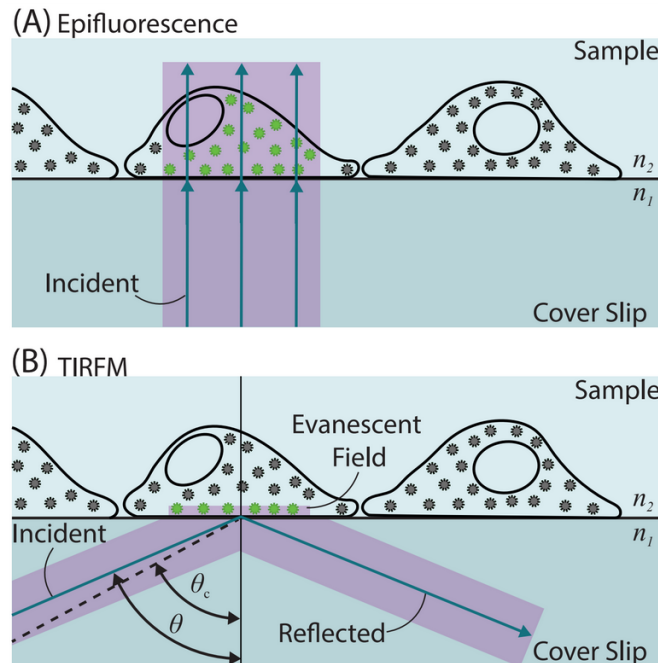


Figure 17

Notably, the evanescent field is spatially short-ranged, typically vanishing over a distance from the interface that is less than a wavelength. In TIRFM, the rapid spatial decay of the evanescent field is key because it ensures that more distant fluorophores are not excited, leading to markedly reduced out-of-focus contamination and markedly enhanced axial discrimination. Alternatively stated, the axial resolution of TIRFM is ~ 100 nm, and this is markedly superior to the axial resolution of conventional diffraction-limited approaches like LSCM. In contrast, the lateral resolution of TIRFM does not exceed the diffraction limit. Photobleaching and phototoxicity also are markedly reduced relative to LSCM.

Cutting-edge super-resolution fluorescence microscopy techniques

TIRFM rose to prominence in the 1980s. More recently, several fluorescence-based techniques have been developed that surpass the diffraction limit in both the lateral and axial directions. These include super-resolution structured

illumination (SR-SIM) and the sequential readout approaches: stimulated emission depletion (STED) microscopy and photoactivated localization microscopy (PALM).

(A) *Super-resolution structured illumination (SR-SIM)*. SR-SIM uses a loop-hole in the diffraction limit to achieve super-resolution. This loop-hole is that the diffraction limit applies directly to the emitted fluorescence signal. However, the fluorophore density is the quantity that is of real experimental interest, and the density can be determined to higher resolution.

SR-SIM is a mathematically complex technique, but the essential idea underlying the approach can be understood by appealing to an analogy with moiré patterns. Consider two relatively closely spaced patterns, one representing the object density and the other the (structured) illumination. Superposition of these can lead to a new moiré pattern, representing the fluorescence signal, that contains a more widely spaced pattern. The key idea of SR-SIM is that this coarser fluorescence pattern might be detectable if its spatial separation is within the diffraction limit. In this case, knowledge of the coarser pattern and the illumination profile, together with application of appropriate mathematical tools, allows detection of closely spaced, otherwise unresolvable details in the density, and the diffraction limit can be surpassed. In the case of SR-SIM, the structured illumination method achieves resolution doubling in the lateral and axial dimensions.

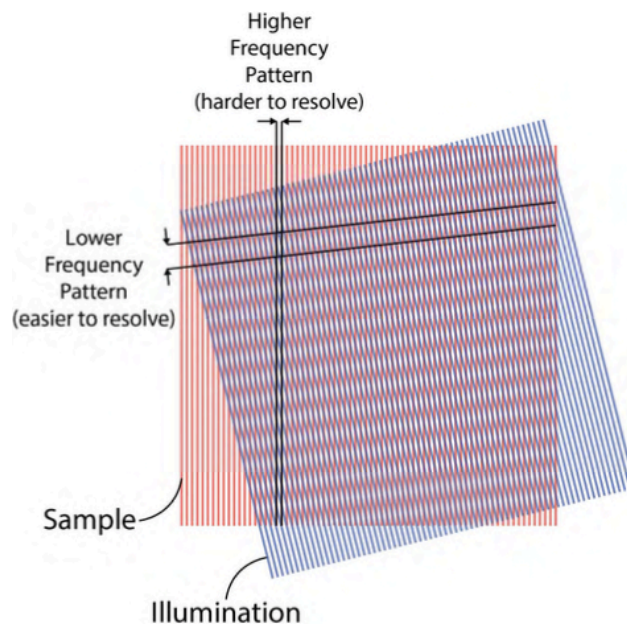


Figure 18

(B) *Sequential readout approaches*. The resolution enhancement in SR-SIM is modest (although significant). A quantum leap in improving the lateral and axial resolution of fluorescence microscopy came with the development of techniques

based on molecular switching and sequential readout. The key idea is that diffraction only precludes resolving closely spaced fluorophores if they are fluorescing (“on”) at the same time because then their diffraction patterns will overlap. Molecular switching and sequential readout bypass the diffraction barrier by ensuring that closely spaced fluorophores are not fluorescing at the same time.

There are a variety of super-resolution techniques that exploit molecular switching and sequential readout. These differ in the methods used to generate, and switch between, bright (on) and dark (off) states and in the methods used to generate fluorophore coordinates. The approaches sometimes are grouped into categories based on whether they involve “targeted switching and readout” or “stochastic switching and readout.” The former approach is used in STED microscopy and the latter approach in PALM.

(B.1) *Targeted switching and readout (STED).* STED commonly is implemented as a point-scanning technique, and thus its enhanced resolution is perhaps best exemplified via comparison with LSCM. To this end, there is a simplistic, but illustrative, analogy. In STED, the scanning spot is engineered to have a width that is roughly an order of magnitude smaller than that of a typical diffraction-limited scanning spot used in LSCM. (This is accomplished by quenching fluorescence in the peripheral region of a diffraction-limited spot using stimulated emission, as shown in Figure 19.) If the scanning spot is regarded as a paint brush, the enhanced resolution obtained with a narrower STED spot can be likened to painting with a narrower brush.

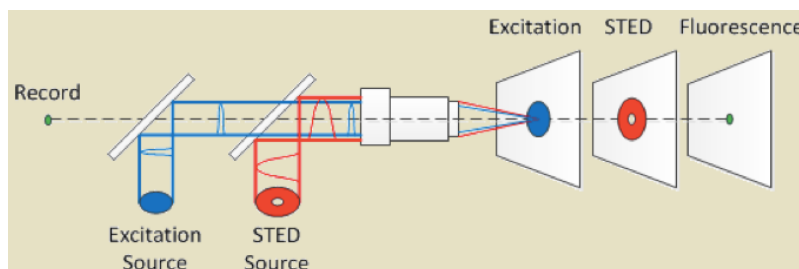


Figure 19

The resolution of STED and LSCM can be compared more rigorously by analyzing how these techniques target and read out fluorophore coordinates. In both methods, fluorophores are excited by a spot, which impinges on a known position, r_i , in the sample. The resulting signals are monitored with a point detector and are assigned to the range of positions occupied by the fluorescing molecules, $r_i \pm \Delta r/2$. The spot is scanned over the sample to build up an image, and the sequentially collected signals map features to a resolution, Δr . Notably, the much smaller spot width in STED leads to markedly enhanced resolution. Currently

realizable resolutions for STED are ~ 20 nm in the lateral direction and ~ 40 nm in the axial direction.

(B.2) *Stochastic switching and readout (PALM).* In PALM, the fluorophores are switched on stochastically, and then the location of each “on” fluorophore is determined. Typically, $\sim 1\%$ of the fluorophores are on simultaneously, which ensures that these fluorophores are separated by more than the diffraction limit and thus that their coordinates can be determined in parallel. Photons emitted by each fluorophore are collected until the fluorophore turns off (e.g., by bleaching) to maximize localization precision and to ensure that there is not a buildup of “on” fluorophores that eventually will cause overlap. The diffraction-limited spot created by each “on” fluorophore is fit to a Gaussian and the center determined to an accuracy of ~ 20 nm. This process is repeated until enough fluorophores are localized to construct an accurate structural representation of the object, as shown in Figure 20. The number of required images is large and is dictated by the need to sample sufficiently finely to meet the requirements of the Nyquist-Shannon sampling theorem. This important theorem states that to achieve a resolution, R , when reconstructing a signal from “samples,” the sample spacing, d , must satisfy $d < R/2$.

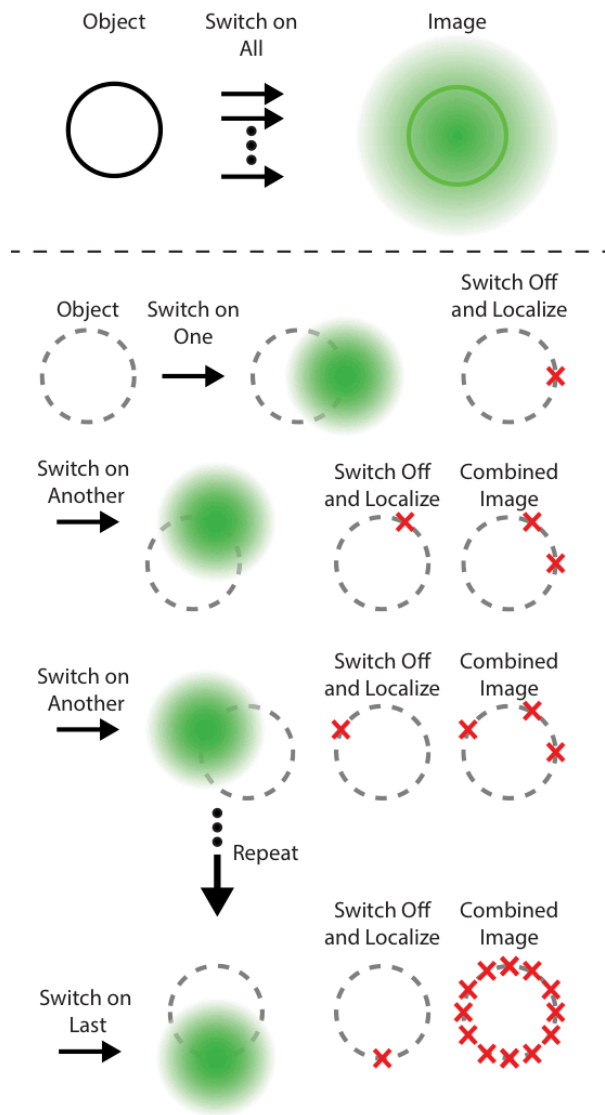


Figure 20